Nanotechnology

DOI: 10.1002/ange.201002037

Self-Assembled Organic Nanostructures with Metallic-Like Stiffness**

Lihi Adler-Abramovich, Nitzan Kol, Inbal Yanai, David Barlam, Roni Z. Shneck, Ehud Gazit, and Itay Rousso**

Organic nanostructures produced by a process of "bottom-up" molecular recognition and self-assembly are key elements in nanotechnology applications. This use of synthetic building blocks with tailored reactivities is highly important for the production of advanced "smart" materials. While these building blocks possess many advantages in terms of synthesis, functionality, and chemical diversity, they usually have inferior mechanical properties compared to metallic nanostructures. Herein we report how indentation-type experiments conducted with an AFM using a diamond-tip cantilever demonstrated remarkable metallic-like point stiffness of up to 885 $N m^{-1}$ and a Young's modulus of up to 275 GPa for aromatic dipeptide nanospheres. This exceptional value makes these nanostructures the stiffest organic materials reported to date (they are even stiffer than macroscopic aramids), thus making them attractive building blocks for the design and assembly of ultrarigid materials with tailored molecular properties. The remarkable stiffness of these assemblies and their transparent optical properties make them ideal elements for the reinforcement of composite materials.

The use of nanostructures for materials reinforcement is one of the most intriguing applications of nanotechnology. This includes far-fetched ideas such as the "space elevator"[1] to realistic objects including reinforced plastic for medical implants or dental materials. Biological material with nanoscale dimensions may have unique mechanical properties, as was demonstrated with spider silk that has a toughness 25 times larger per weight than that of steel.[2] While there has been much effort in the development of self-assembled protein and peptide nanomaterials,[3] these bioinspired assemblies are usually significantly less rigid than metallic structures.

We probed the mechanical properties of nanospheres, which are formed by the self assembly of the Boc-Phe-Phe-OH peptide (Boc = *tert*-butoxycarbonyl, Phe = phenylalanine), a member of the aromatic dipeptide structural family that can form various nanoscale structures.[4] A phase diagram of the Boc-Phe-Phe-OH building block defines its assembly into a homogeneous population of either spherical or tubular nanostructures.[4c,5] We used indentation-type experiments with AFM to study the mechanical properties of the spheres as this technique has a combination of low penetration depths and high lateral precision, which make it a powerful and attractive tool to measure the mechanical properties of nanoscale biological structures.[6] AFM has indeed been used to study the specific interactions of biomolecules at the single-molecule level by utilizing antibody–antigen interactions.[7]

The Boc-Phe-Phe-OH peptide was dissolved in hexafluoro-2-propanol at a concentration of 100 $mg mL^{-1}$ and then diluted with ethanol to form the spheres. The spheres were deposited on a mica surface and imaged using AFM (Figure 1a) and SEM (Figure 1b). We analyzed the size distribution of nearly 15000 spheres from the SEM images. The spheres' size varied from 30 nm to 2 μm in diameter and was distributed as shown in Figure 1c.

The mechanical properties of the peptide nanospheres were measured by positioning the AFM tip at the center of a single sphere surface and acquiring force–distance curves at that position. The first experiment carried out with a metallic AFM cantilever already demonstrated the remarkable rigidity of these structures, as no deformation could be observed. Therefore, force–distance experiments were conducted after switching to a diamond cantilever with a spring constant of more than 350 $N m^{-1}$. A typical force–distance curve and a corresponding cantilever deflection curve are shown in Figure 2a. The cantilever deflection graph is obtained by measuring a force–distance curve for mica, and the loading force is calculated by multiplying the cantilever deflection reading by the cantilever spring constant. The difference for a given loading force between the z displacements of the tip on the peptide nanospheres and on the mica is

[*] L. Adler-Abramovich,[+] I. Yanai, Prof. E. Gazit
Department of Molecular Microbiology and Biotechnology
George S. Wise Faculty of Life Sciences
Tel Aviv University, Tel Aviv 69978 (Israel)
E-mail: ehudg@post.tau.ac.il
N. Kol,[+] Prof. I. Rousso
Department of Structural Biology, Weizmann Institute of Science
Rehovot 76100 (Israel)
E-mail: itay.rousso@weizmann.ac.il
Prof. D. Barlam
Department of Mechanical Engineering
Ben-Gurion University of the Negev (Israel)
Prof. R. Z. Shneck
Department of Materials Engineering
Ben-Gurion University of the Negev (Israel)
[+] These authors contributed equally to this work.

[**] We thank Dr. Ellen Wachtel for help with the XRD analysis, Prof. Yeshayahu Talmon for help with the ED analysis, Dr. Zahava Barkay for help with the SEM analysis, Prof. Reshef Tenne and Ofer Tevet for the use of the HR-SEM equipped with nanomanipulator, and members of the Gazit laboratory for helpful discussions. L.A.A. gratefully acknowledges the support of the Colton Foundation. I.R. holds the Robert Edwards and Roselyn Rich Manson Career Development Chair. We thank the Israel Science Foundation for financial support.

Supporting information (including detailed experimental procedures) for this article is available on the WWW under http://dx.doi.org/10.1002/anie.201002037.

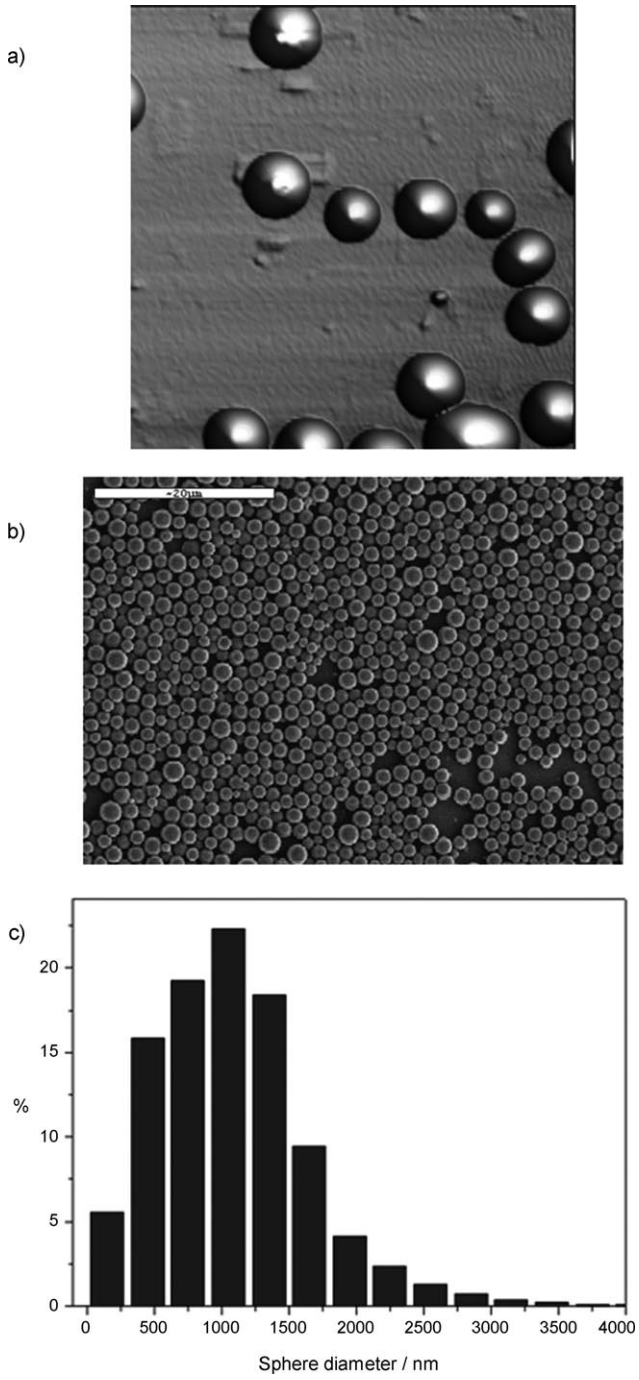

Figure 1. Analysis of Boc-Phe-Phe-OH peptide spheres of different sizes. a) AFM images of nanospheres deposited on freshly cleaved mica (scan area 10×10 μm, 512×512 pixels). b) SEM micrograph of the nanospheres exhibits their size distribution. Scale bar 20 μm. c) Size distribution of 14885 peptide spheres.

the indentation of the nanospheres by the AFM probe. The point stiffness was calculated as previously described.[8]

To exclude possible irreversible deformation of the nanospheres during around 100 repeated force–distance curves, the measured point stiffness was plotted as a function of the measurement number (Figure 2a, inset). During each experiment, the stiffness values obtained from the individual force curves were found to distribute normally around a mean

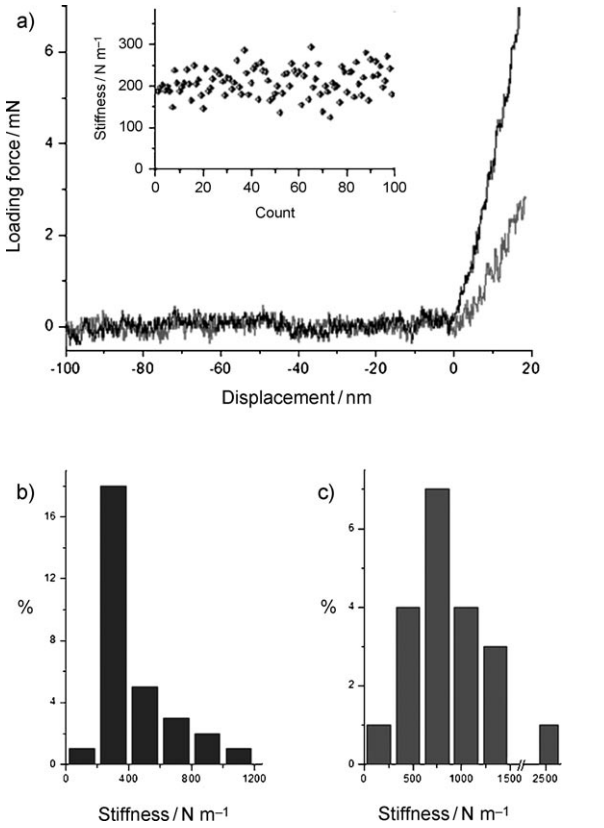

Figure 2. Measurements of the point stiffness of the peptide spheres. a) Typical force–distance curve of a peptide nanosphere (gray curve) in reference to the cantilever deflection curve (black curve). The inset shows a scatter plot of the individual measured point stiffness values obtained for the sphere as a function of the experimental number (count). Sphere stiffness distribution b) columns show the spheres with diameters of approximately 200 nm (mean = 430; $n = 30$); c) columns show spheres with diameters of approximately 1 μm (mean = 885; $n = 20$).

value, thus suggesting that the nanosphere did not undergo irreversible deformation. In addition, calculation of the spheres' stiffness using the loading or unloading curves results in a small average difference of 15%, which further supports the elastic nature of the indentation experiment.

The distributions of calculated point stiffness values for nanospheres with a diameter of approximately 200 nm ($n = 30$) and 1 μm ($n = 20$) are shown in Figure 2b and c, respectively. The average stiffness of a 200 nm sphere was calculated to be 430 $N\,m^{-1}$, and the average stiffness of a 1 μm sphere was calculated to be 885 $N\,m^{-1}$. The difference between these stiffness values is likely due to the known dependency of point stiffness on sample dimensions rather than representing a difference in the inherent properties of the material related to the multiwalled structure of the nanospheres. An imprint of the indenter at the nanosphere surface or a complete collapse of the structure were rarely detected in the images taken at the end of the indentation experiment (Figure S3 in the Supporting Information). While these particular experiments were not used for calculating the nanospheres' stiffness, they excluded the possibility of deposition of the tip to the surface.

To further support our stiffness results, we performed indentation measurements inside a high-resolution scanning electron microscope (HR-SEM) equipped with a nanomanipulator.[9] The deformation of the nanosphere can be directly visualized with this setup. No deformation was observed when a 40 N m^{-1} cantilever was applied with maximum pressure to the spheres, as is consistent with our AFM measurements.

Unfortunately, there is no suitable mathematical model that can be used to convert the measured stiffness to Young's modulus. We therefore performed finite-element simulations to estimate the spheres' material properties from their stiffness values. In the simulation, a model sphere was indented and the corresponding stiffness was derived from the ratio between the applied force and the displacement. We assumed that the mechanical behavior of the spheres can be described as linear elastic, which is a good approximation for solids under small strains. The Young's modulus of the simulated sphere was changed consistently until the simulated stiffness was in good agreement with its experimental counterpart. The results are dependent to a large extent on the accurate modeling of the geometry of the spheres, that is, size and internal structure. The size distribution of the spheres was determined from SEM images and two representative size values were chosen accordingly (200 nm and 1 μm). The internal structure of the spheres contains a cavity, as was confirmed by electron microscopy images that show the inclusion of nanoparticles during self-assembly in the presence of those smaller particles (data not shown).

We were unable to determine the size of the inner cavity and therefore modeled two extreme cases. In the first model, the spheres' shells had thickness comprising 80% of its radius. In the second model, the shell thickness was reduced to 20% of the spheres' radii. Figure 3 shows the deformed and undeformed shapes of the two models. The fitting of the elastic moduli for the simulated thick shell sphere gives a Young's modulus of $E \approx 230$ GPa for the particle with a diameter of 200 nm, and a value of approximately 275 GPa, for the 1 μm sphere. For a thin-walled sphere, the fitting yields a Young's modulus of $E \approx 140$ GPa and approximately 230 GPa for the 200 nm and 1 μm spheres respectively (Table 1). Regardless of sphere size, the Young's modulus obtained for the thin shell is lower than the corresponding thick-shell value. This result is primarily due to the larger contribution of the overall structural deformation to its stiffness in the case of the thin shell (Figure 3). In the case of the thick shell, deformation and stresses are local in nature, however, in the case of the thin shell, a large segment of the entire structure moves during the indentation process. Part of the applied load is diverted into this movement giving the appearance of a stiffer response than would be expected based on the mechanical properties of the shell alone. Thus a lower Young's modulus value is required for these experiments.

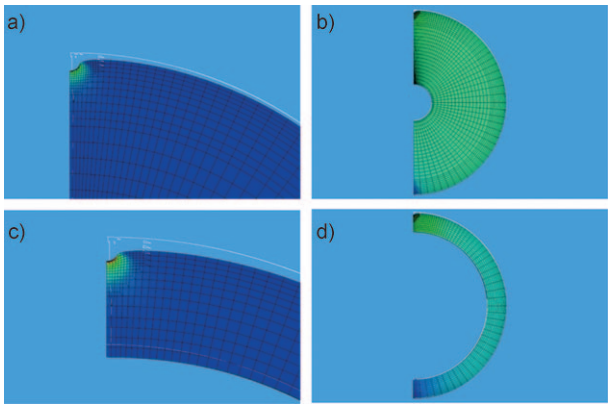

Figure 3. Finite element simulation for indentation of a sphere. a, b) Deformed and undeformed shape of a thick ($t/R = 0.8$) wall sphere respectively, where t is the wall thickness and R is the external radius of the sphere. c, d) Deformed and undeformed shape of a ($t/R = 0.2$) thin-wall sphere respectively. The contours of the sphere prior to the indentation are shown by white lines.

Table 1: Finite element analysis.

Particle diameter	Stiffness [N/m]	E [GPa][a]	
		10%	40%
200 nm	430	140	230
1 μm	885	230	275

[a] Assuming inner-shell thickness of 10% or 40%.

An important question that must be addressed is related to the effect that the content of the nanospheres' cavities may have on their Young's modulus. We therefore modeled these nanospheres as empty particles or filled with noncompressible water. Regardless of whether the cavity is empty or water-filled, the obtained Young's modulus remained unchanged. This result is expected for a sphere made from a material with such an extremely high stiffness.

Previous studies presented the mechanical strength of the diphenylalanine peptide nanotubes. Direct AFM measurements had indicated an average point stiffness of 160 N m^{-1} and Young's modulus of about 20 GPa for peptide nanotubular assemblies.[8] A similar Young's modulus value ((27 ± 4) GPa) was obtained in an independent study.[10] Therefore, we suggest that a novel method for material reinforcement could be achieved by the combination of the peptide nanospheres, which possess the notable mechanical characteristics that were presented in this study, together with the peptide nanotubes. Aligned peptide nanotubes could increase the bending rigidity while the nanospheres could increase the pressing rigidity similar to the role of aligned metal bars and crushed stones in concrete.

The calculated Young's modulus is significantly higher than calculated for any organic material. As a reference, the calculated Young's moduli for protein structures of the dragline spider silk and the silkworm *Bombyx mori* silk mentioned above is 10 GPa and 8 GPa respectively.[2c] These spherical structures are also stiff compared to steel (ca. 200 GPa) and carbon fibers (ca. 300 GPa).[2a]

To investigate the structural basis for the rigidity of the spherical nanostructures, we carried out X-ray diffraction (XRD) analysis. Data collection was performed in the $\theta/2\theta$ mode (Figure S1 in the Supporting Information). The XRD patterns of the spheres exhibit a number of relatively weak

diffraction peaks, which indicate that the Boc-Phe-Phe-OH peptide spheres display some degree of crystalline order, although the degree of crystallinity is lower than that of the diphenylalanine peptide nanotubes reported previously.[11] Electron diffraction measurements were carried out at approximately −180 °C on the nanospheres (Figure S2 in the Supporting Information). The results revealed diffuse rings rather than discrete diffraction peaks and are consistent with a lower degree of order than that of the nanotubes.[11b] This result is quite remarkable when taking into account that the Young's modulus of the nanospheres is at least tenfold higher than that of the nanotubes. The molecular basis for this phenomenon is intriguing, and may be related to the observation of increased rigidity in amorphous steel as compared to more ordered metals and alloys.[12] The marked increase in rigidity of the spherical assemblies could not be based only on the geometry of nanoassemblies but should reflect additional bonding that stabilizes the supramolecular systems. As was previously suggested for cationic systems, additional bond between headgroups (such as a hydrogen bond between parallel carboxylate groups)[13] could provide further bending rigidity by a lateral interaction network.[14] Indeed, in the case of Boc-Phe-Phe-OH, in which the amine moiety is blocked and only the carboxyl group is available for further interactions, the geometrically restricted orientation of the building blocks that results from π–π interactions[4a,b,15] may lead to a parallel orientation of the Boc-Phe-Phe-OH building blocks and the formation of a surface in which the carboxylate moieties form a network of lateral hydrogen bonds. As was previously suggested, such a network at could be modeled at the mesoscopic scale as a spring network that provides additional bending rigidity.[14b]

The remarkable rigidity of both tubular and spherical aromatic dipeptide nanostructures resembles that of the polymeric aramids such as Kevlar. As with the aromatic polyamides, the combination of the geometrically restricted π–π interactions between the aromatic moieties[11a] together with the planar nature of the amide bond may provide the unique mechanical properties so rarely observed in organic materials. If Kevlar is compared to its non-aromatic polyamide analogues, such as nylon, the role of the aromatic interactions is evident.[16] As with the aromatic Kevlar, we expect that the peptide nanostructures described here may open new directions towards the development of organic nanotechnology. As a reference, Kevlar 49 fibers have a Young's modulus of around 130 GPa.[17]

We have demonstrated the remarkable and unprecedented rigidity of organic self-assembled nanostructures with a Young's modulus in the range of hundreds of GPa. The mechanical properties of these spherical assemblies and their transparent optical properties suggest that they will be ideal elements for the reinforcement of various materials such as composite materials.[18] The combination of the tubular and spherical assemblies will enable reinforcement of both bending and pressing rigidity for applications in a wide range of fields including plastics reinforcement, biomaterials for implant and dental applications, aviation, space, and other applications that require inexpensive, lightweight organic materials with remarkable rigidity and exceptional stability.

Received: April 6, 2010
Revised: August 22, 2010
Published online: September 28, 2010

Keywords: mechanical strength · nanostructures · nanotechnology · peptides · self-assembly

[1] N. M. Pugno, F. Bosia, A. Carpinteri, *Small* **2008**, *4*, 1044
[2] a) J. M. Gosline, P. A. Guerette, C. S. Ortlepp, K. N. Savage, *J. Exp. Biol.* **1999**, *202*, 3295; b) F. Vollrath, D. P. Knight, *Nature* **2001**, *410*, 541; c) M. Heim, D. Keerl, T. Scheibel, *Angew. Chem.* **2009**, *121*, 3638; *Angew. Chem. Int. Ed.* **2009**, *48*, 3584.
[3] a) I. A. Banerjee, L. Yu, H. Matsui, *Proc. Natl. Acad. Sci. USA* **2003**, *100*, 14678; b) M. R. Ghadiri, J. R. Granja, R. A. Milligan, D. E. McRee, N. Khazanovich, *Nature* **1993**, *366*, 324; c) J. D. Hartgerink, E. Beniash, S. I. Stupp, *Proc. Natl. Acad. Sci. USA* **2002**, *99*, 5133; d) S. Vauthey, S. Santoso, H. Gong, N. Watson, S. Zhang, *Proc. Natl. Acad. Sci. USA* **2002**, *99*, 5355; e) A. Aggeli, M. Bell, N. Boden, J. N. Keen, P. F. Knowles, T. C. McLeish, M. Pitkeathly, S. E. Radford, *Nature* **1997**, *386*, 259.
[4] a) M. Reches, E. Gazit, *Science* **2003**, *300*, 625; b) M. Reches, E. Gazit, *Nano Lett.* **2004**, *4*, 581; c) M. Reches, E. Gazit, *Isr. J. Chem.* **2005**, *45*, 363; d) M. Reches, E. Gazit, *Phys. Biol.* **2006**, *3*, S10.
[5] L. Adler-Abramovich, E. Gazit, *J. Pept. Sci.* **2008**, *14*, 217.
[6] A. del Rio, R. Perez-Jimenez, R. Liu, P. Roca-Cusachs, M. J. Fernandez, P. M. Sheetz, *Science* **2009**, *323*, 638.
[7] C. Stroh, H. Wang, R. Bash, B. Ashcroft, J. Nelson, H. Gruber, D. Lohr, S. M. Lindsay, P. Hinterdorfer, *Proc. Natl. Acad. Sci. USA* **2004**, *101*, 12503.
[8] N. Kol, L. Adler-Abramovich, D. Barlam, R. Z. Shneck, E. Gazit, I. Rousso, *Nano Lett.* **2005**, *5*, 1343.
[9] O. Tevet, O. Goldbart, S. R. Cohen, R. Rosentzveig, R. Popovitz-Biro, H. D. Wagner, R. Tenne, *Nanotechnology* **2010**, *21*, 365705.
[10] L. Niu, X. Chen, S. Allen, S. J. B. Tendler, *Langmuir* **2007**, *23*, 7443.
[11] a) C. H. Gorbitz, *Chem. Commun.* **2006**, 2332; b) M. Reches, E. Gazit, *Nat. Nanotechnol.* **2006**, *1*, 195.
[12] X. J. Gu, S. J. Poon, G. J. Shiflet, M. Widom, *Acta Mater.* **2008**, *56*, 88.
[13] M. L. Lynch, Y. Pan, R. G. Laughlin, *J. Phys. Chem.* **1996**, *100*, 357.
[14] a) N. Delorme, M. Dubois, S. Garnier, A. Laschewsky, R. Weinkamer, T. Zemb, A. Fery, *J. Phys. Chem. B* **2006**, *110*, 1752; b) M. A. Hartmann, R. Weinkamer, T. Zemb, F. D. Fischer, P. Fratzl, *Phys. Rev. Lett.* **2006**, *97*, 018106; c) M. Dubois, B. Deme, T. Gulik-Krzywicki, J.-C. Dedieu, C. Vautrin, S. Desert, E. Perez, T. Zemb, *Nature* **2001**, *411*, 672.
[15] a) E. Gazit, *FASEB J.* **2002**, *16*, 77; b) C. A. Hunter, J. Singh, J. M. Thornton, *J. Mol. Biol.* **1991**, *218*, 837; c) C. A. Hunter, J. K. M. Sanders, *J. Am. Chem. Soc.* **1990**, *112*, 5525.
[16] E. Gazit, *Chem. Soc. Rev.* **2007**, *36*, 1263.
[17] http://www2.dupont.com/Kevlar/en_US/index.html.
[18] P. M. Ajayan, J. M. Tour, *Nature* **2007**, *447*, 1066.

